

Synthesis of Aluminum Oxide/Gradient Copolymer Composites by Atom Transfer Radical Polymerization

Bin Gu and Ayusman Sen*

Department of Chemistry, The Pennsylvania State University, University Park, Pennsylvania 16802

Received May 24, 2002

Revised Manuscript Received August 20, 2002

Introduction

The development of strategies for the synthesis of novel ceramic/polymer composites is of great current interest because of the unique properties that are likely to emerge from such materials.^{1–11} One of the most important challenges in the area is the synthesis of composites where the polymer chains are covalently bonded to the ceramic particles and where the composition and the length of the chains can be varied in a systematic way. The optimum solution to this problem is a living polymerization system that initiates from the surface of the ceramic particles, such as by atom transfer radical polymerization (ATRP).¹² To date, ATRP has been employed to anchor homopolymers on to silica, cadmium sulfide/silica, and gold particle surfaces.^{13–16} There are no reports of the use of metal oxides in such procedures, and there is no precedent for the ATRP synthesis of copolymers from ceramic surfaces. Thus, there were two unanswered questions: (a) Do copolymerizations follow the living characteristics of liquid-phase ATRP? (b) Can copolymer compositions be predicted from monomer reactivity ratios determined from liquid-phase radical polymerizations?

Herein we report the synthesis of gradient poly-(methyl methacrylate)-*co*-poly(butyl acrylate) (PMMA-*co*-PBA) copolymer chains from the surface of aluminum oxide particles by ATRP using the CuBr/PMDETA catalyst system (Figure 1). The oxide particles can act as cross-linking sites, leading to improved mechanical and thermal properties for the polymer. In addition, the procedure renders the oxide particles hydrophobic and makes them more compatible with a polymer matrix, resulting in more homogeneous ceramic/polymer blends.⁶ The polymeric coat also prevents agglomeration of the particles and allows higher loading levels in such blends.

Experimental Section

Materials. CuBr (99.999%), *N,N,N,N,N'*-pentamethyldiethylenetriamine (PMDETA, 99%), 2-bromopropionic acid (99%), tetrahydrofuran (THF, 99.9%), and chloroform (99.9%, HPLC grade) were obtained from Aldrich and used as received. Methyl methacrylate (MMA) (99%, Aldrich) and butyl acrylate (BA, 99%, Aldrich) were vacuum-distilled from CaH₂ and stored under N₂. Aluminum oxide was purchased from Nanophase, Inc. According to specifications, the size of the particles range from 27 to 56 nm. However, SEM (Figure 7a) indicates that the particles form agglomerates.

Analysis. NMR spectra were recorded on a Bruker DPX-300 spectrometer. The chemical shifts are referenced to CHCl₃. Molecular weights and molecular weight distributions were determined on a Waters size exclusion chromatography (SEC)

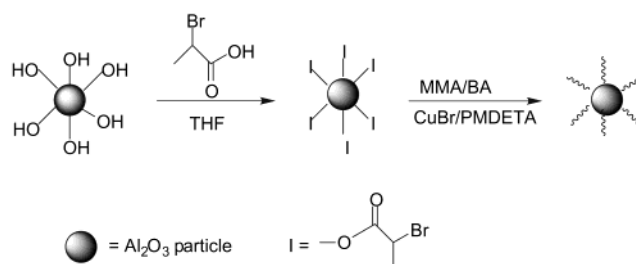


Figure 1. Synthetic route to Al₂O₃/PMMA-*co*-PBA composites

system using a flow rate of 1 mL/min and a three-column bed (Styragel HR 7.8 × 300 mm columns with 5 μm bead size: 100–10 000, 500–30 000, and 5000–6 000 000 Da), a Waters 410 differential refractometer, and a Waters 486 tunable absorbance detector. SEC samples were run in CHCl₃ at ambient temperature and calibrated to polystyrene standards. Elemental analysis was provided by Galbraith Laboratories. IR spectra were recorded on a Perkin-Elmer 1600 FT-IR spectrophotometer using KBr pellets. Scanning electron micrographs (SEM) were obtained on a JSM 5400 instrument. Differential scanning calorimetry was performed on Perkin-Elmer DSC-7 under an argon atmosphere at a scanning rate of 5 °C/min.

Modification of Aluminum Oxide Particles with Initiator. A mixture of Al₂O₃ (2.04 g, 0.02 mol), 2-bromopropionic acid (3.04 g, 0.02 mol), and 30 mL of THF was heated to reflux for 15 h. After filtration, excess acid was washed away with acetone, and volatile materials were removed under vacuum. The successful anchoring of the initiator was verified by bromine analysis which gives a bromine content of 0.57%.

Polymerization of MMA and BA from Particle Surfaces. In a typical reaction, 0.47 g of initiator modified particles, CuBr (43 mg, 0.30 mmol), PMDETA (52 mg, 0.30 mmol), MMA (1.00 g, 0.01 mol), BA (1.28 g, 0.01 mol), and 0.10 mL of DMSO (internal standard) were degassed by freeze–pump–thaw cycles before being filled with N₂. After polymerizing at 110 °C for 4 h, the flask was cooled in ice to stop the reaction, and products were suspended in chloroform. DOWEX MSC-1 ion-exchange resin was added to remove the copper catalyst, and the suspension became white. After removing the ion-exchange resin and evaporating the solvent, a white solid was obtained. Yield: 1.91 g. IR (KBr, cm^{−1}): 3441, 2900, 1738.

For kinetic studies, samples were taken from the reaction at 1 h intervals, filtered, and dissolved in CDCl₃. The conversions of MMA and BA were calculated from the integration of vinylic hydrogens of unreacted monomers relative to DMSO internal standard. The specific chemical shifts used were 5.55 ppm (1H, MMA) and 6.37 ppm (1H, BA). For film casting, the composites were suspended in CHCl₃ and added to a glass plate dropwise. Film formed upon evaporation of solvent.

Cleavage of Polymer from Alumina Particles. Polymer chains were cleaved from the particles by treatment with HF following the procedure described previously.¹³ In a typical procedure, alumina/polymer composite (0.40 g) was suspended in 10 mL of chloroform, and 100 mg of Aliquot 336 was added as a phase transfer catalyst. A 10 mL aliquot of 5% aqueous HF was then added, and the mixture was stirred at ambient temperature for 2 h. The organic layer was removed, and polymer was isolated by precipitation in methanol. ¹H NMR (CDCl₃, ppm): 0.8–2.0, 3.6 (OCH₃, MMA), 4.1 (OCH₂, BA). *M_n* = 51 000. *M_w*/*M_n* = 1.31.

Results and Discussion

Modification of Aluminum Oxide Particles. Previous work on ATRP from silica, cadmium sulfide/silica, and gold particles employed noncommercially available initiators that bind to the surface of these particles.^{13–16}

* To whom correspondence should be addressed. E-mail: asen@psu.edu.

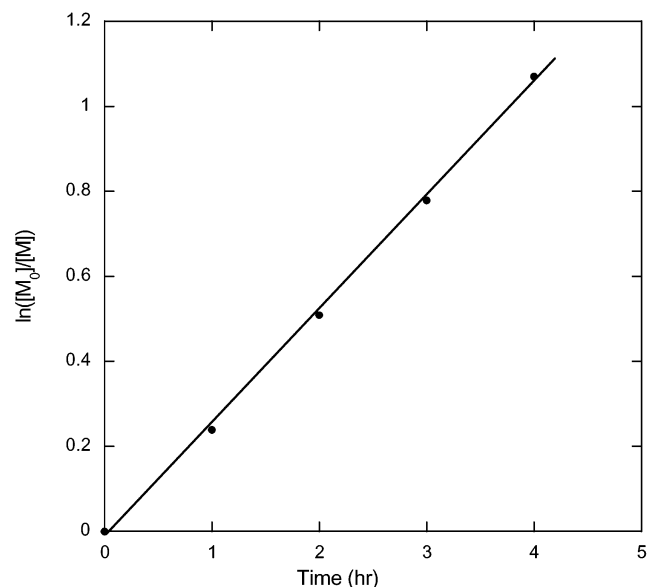


Figure 2. Kinetics of copolymerization of MMA and BA from modified Al_2O_3 particles. Conditions: $[\text{MMA}]_0 = [\text{BA}]_0 = 0.01$ mol; modified Al_2O_3 particles, 0.47 g; $[\text{CuBr}] = [\text{PMDETA}] = 0.30$ mmol; 110°C .

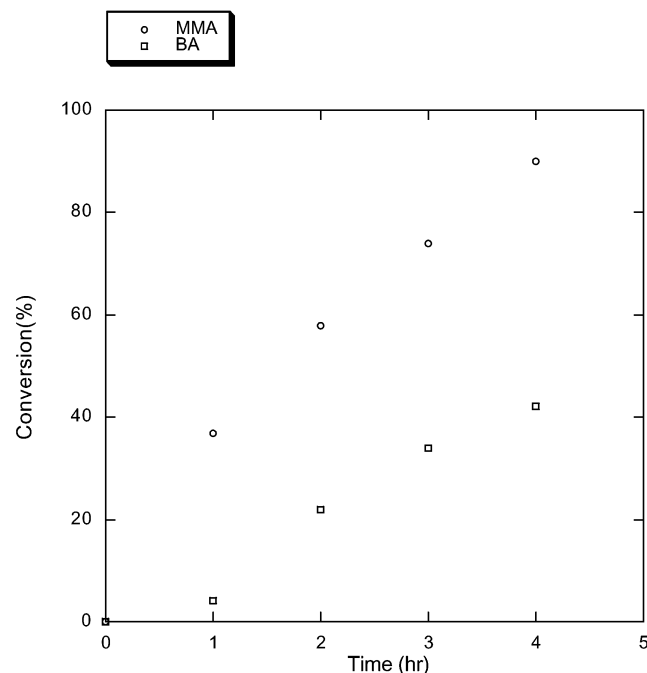


Figure 3. Conversion of MMA and BA with time. Conditions: $[\text{MMA}]_0 = [\text{BA}]_0 = 0.01$ mol; modified Al_2O_3 particles, 0.47 g; $[\text{CuBr}] = [\text{PMDETA}] = 0.30$ mmol; 110°C .

We found that the readily available 2-bromopropionic acid can react with the hydroxyl groups on aluminum oxide surface to afford particles incorporating initiators for ATRP.

Kinetics and Mechanism of Polymerization Initiated from Aluminum Oxide Particles. We sought to compare the characteristics of ATRP copolymerization initiated from a ceramic surface with that observed in liquid-phase. On the basis of the initiator concentration obtained by bromine analysis, a monomer/initiator ratio $\sim 10^2$ was chosen for the copolymerization experiments. The conversions of MMA and BA were calculated from the integration of vinylic hydrogens of unreacted monomers relative to DMSO internal standard.

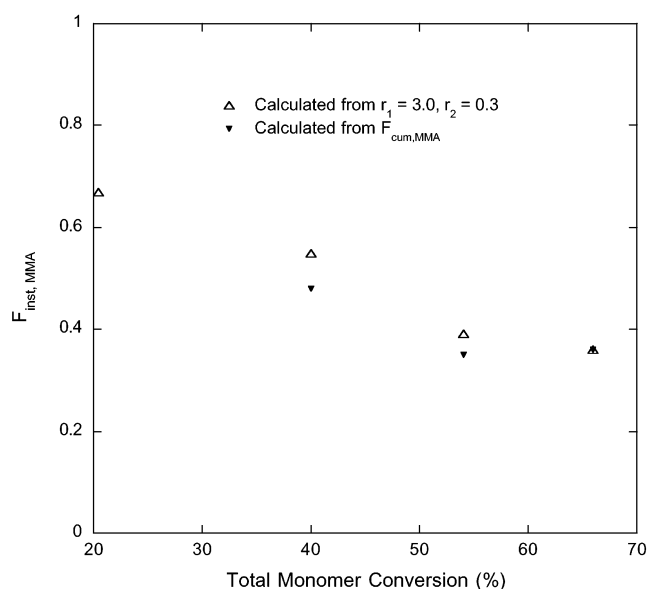


Figure 4. Instantaneous copolymer composition vs monomer conversion. Conditions: $[\text{MMA}]_0 = [\text{BA}]_0 = 0.01$ mol; modified Al_2O_3 particles, 0.47 g; $[\text{CuBr}] = [\text{PMDETA}] = 0.30$ mmol; 110°C .

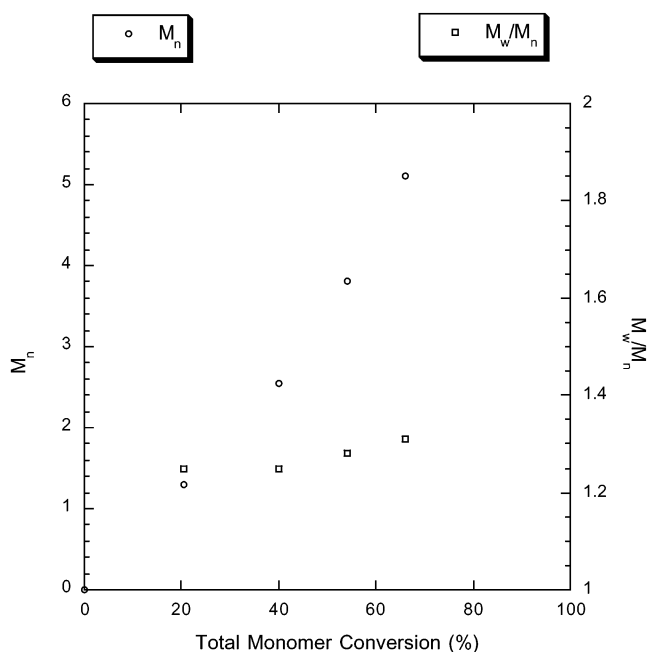


Figure 5. Molecular weight and polydispersity of PMMA-co-PBA as a function of conversion. Conditions: $[\text{MMA}]_0 = [\text{BA}]_0 = 0.01$ mol; modified Al_2O_3 particles, 0.47 g; $[\text{CuBr}] = [\text{PMDETA}] = 0.30$ mmol; 110°C .

As shown in Figure 2, the polymerization exhibited first-order kinetics with respect to total monomer conversion. Similar first-order kinetics were also observed for the conversions of the individual monomers.

Matyjaszewski has studied the liquid-phase copolymerization of MMA and BA using the $\text{CuBr}/\text{PMDETA}$ catalyst system and methyl 2-bromopropionate as the initiator.¹⁷ Because of its higher reactivity ratio, the uptake of MMA is faster than that of BA. For equimolar monomer feed ratio, 70% of total monomer conversion was reached after 3.6 h. With the $\text{NiBr}_2(\text{P}^n\text{Bu}_3)_2/\text{Al}(\text{O}^i\text{Pr})_3/\text{CCl}_3\text{Br}$ system, MMA was also consumed faster than BA.¹⁸ As shown in Figure 3, the same trend is observed in the present case. For example, after 4 h

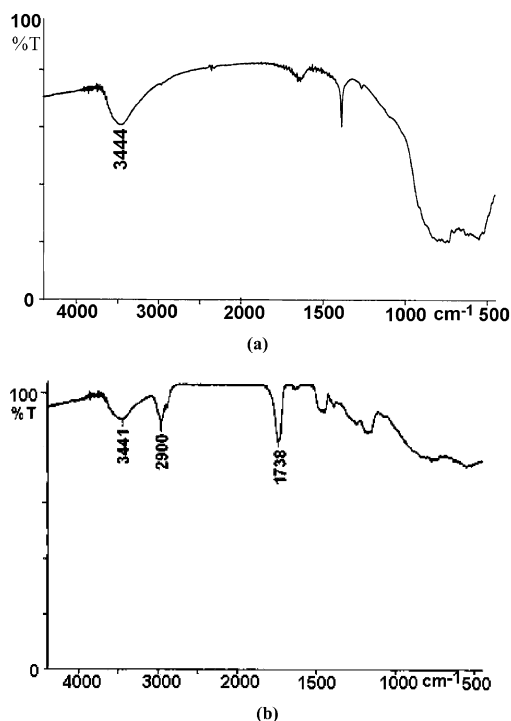


Figure 6. FT-IR (KBr) spectra of (a) untreated Al_2O_3 particles and (b) Al_2O_3 /PMMA-co-PBA composite.

approximately 90% of MMA was consumed while only about 40% BA had reacted (65% total monomer conversion). A higher reaction temperature was employed due to the heterogeneity of the reaction mixture. There was no polymer found in solution after removal of the alumina particles, suggesting that the formed polymer chains were attached to the alumina surface.

The data in Figure 3 can also be used to calculate the instantaneous copolymer composition at any given monomer conversion. First, the cumulative copolymer composition is obtained from eq 1, where subscript 1 denotes the first monomer (MMA) and subscript 2 denotes the second monomer (BA). The instantaneous composition is then obtained from eq 2.¹⁷ The values obtained can be compared with theoretical instantaneous compositions obtained using eq 3,¹⁹ and the reactivity ratios can be measured from liquid-phase

polymerization reactions ($r_1 = 3.0$ for MMA, $r_2 = 0.3$ for BA¹⁷).

$$F_{\text{cum},1} = \frac{(\% \text{ conv})_1 [\text{M}_1]_0}{(\% \text{ conv})_1 [\text{M}_1]_0 + (\% \text{ conv})_2 [\text{M}_2]_0} \quad (1)$$

$$F_{\text{inst},1} = F_{\text{cum},1} + (\% \text{ conv}) \frac{\Delta F_{\text{cum},1}}{\Delta (\% \text{ conv})} \quad (2)$$

$$F_{\text{inst},1} = \frac{r_1 f_1^2 + f_1 f_2}{r_1 f_1^2 + 2 f_1 f_2 + r_2 f_2^2} \quad (3)$$

where f_1 and f_2 are the instantaneous monomer fractions.

As shown in Figure 4, the two sets of values agree well, suggesting that the reactivity ratios obtained from liquid-phase polymerizations can be used to predict the compositions of copolymers grown on ceramic surfaces. Figure 4 also shows that we have controlled *gradient* copolymer chains that are MMA rich near the surface and become progressively richer in BA content on going further out. This observation suggests further ways to synthesize novel ceramic/polymer architectures.

To measure the molecular weight and polydispersity of the copolymer chains, they were cleaved off the alumina surface using HF and analyzed by GPC. Figure 5 shows plots of M_n and M_w/M_n as a function of total monomer conversion. For M_n , the plot deviates from linearity at higher conversions due to differential uptake of the two monomers. Starting with an equimolar monomer feed ratio, the more reactive MMA is preferentially incorporated at the beginning, thus making the monomer composition progressively richer in the less reactive BA. The polydispersity remains fairly low throughout, suggesting that the polymerization is "living". The narrow, monomodal, distribution also confirms that the chains are copolymers rather than mixtures of homopolymers.

The theoretical M_n for the copolymer can be calculated from the $[\text{MMA} + \text{BA}]_0$:[initiator] ratio and the conversion of each monomer. For example, at 90% of MMA and 40% BA conversion (65% total monomer conversion), the theoretical M_n is 43 000. The corresponding M_n value obtained by GPC relative to polystyrene

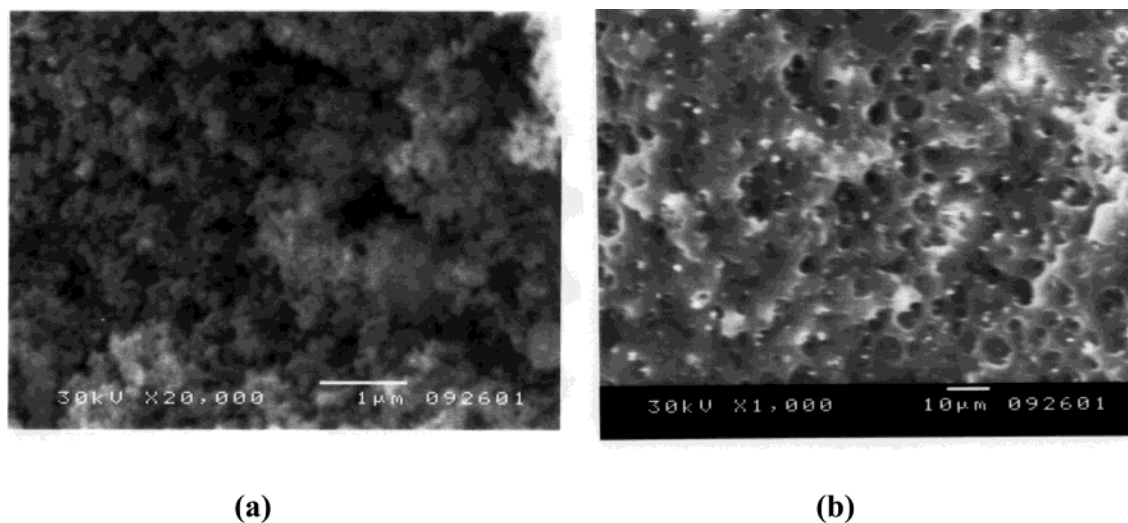


Figure 7. SEM of (a) untreated Al_2O_3 particles and (b) Al_2O_3 /PMMA-co-PBA composite film prepared by casting from CHCl_3 .

standards is 51 000. The similarity of the numbers suggests that most of the initiation sites on the alumina particles participate in ATRP.

Characterization of the Aluminum Oxide/Copolymer Composites. IR spectra of the pure Al_2O_3 particles and Al_2O_3 /PMMA-*co*-PBA composite ($M_n \sim 51\,000$) are shown in Figure 6. The characteristic absorption band of C=O at 1738 cm^{-1} corresponding to the ester groups in the polymer can be observed after PMMA-*co*-PBA is grown from the alumina particles. The presence of an absorption band at 3440 cm^{-1} in the Al_2O_3 /PMMA-*co*-PBA composite indicates that all of the surface hydroxyl groups on the alumina particles did not participate in the reaction with 2-bromopropionic acid.

Scanning electron micrographs (SEM) of starting Al_2O_3 particles and Al_2O_3 /PMMA-*co*-PBA composite film ($M_n \sim 51\,000$) are shown in Figure 7. According to manufacturer's specifications, the size of the particles range from 27 to 56 nm. However, SEM (Figure 7a) indicates that the particles form agglomerates. Such agglomerates are formed to lower total surface energy.²⁰ After polymerization, the agglomerates are broken up and the particles (bright dots) distributed homogeneously in the copolymer matrix. The particles are mostly $1\text{ }\mu\text{m}$ in size and are embedded in the polymer matrix. The initial particle agglomeration evidently prevented reaction of all of the surface hydroxyl groups with 2-bromopropionic acid.

While the initial alumina particles settled out rapidly from organic solvents, the alumina/PMMA-*co*-PBA composite ($M_n \sim 51\,000$) formed a stable colloidal suspension in chloroform, acetone, and toluene. Clearly, this is the result of the increased hydrophobicity of the ceramic surface in the composite.

Finally, the Al_2O_3 /PMMA-*co*-PBA composite ($M_n \sim 51\,000$) was examined by differential scanning calorimetry (DSC). No glass transition was observed in the temperature range $0\text{--}300\text{ }^\circ\text{C}$.

Conclusion

Aluminum oxide particles can be conveniently modified to afford surface initiation sites for ATRP. Copolymer chains with controlled composition and length can be grown from the particle surface. The copolymerization process is living and follows the same trends as is observed in liquid-phase ATRP. This allows the synthesis of controlled gradient copolymer chains that are richer in one monomer near the particle surface and

become progressively richer in the other monomer on going further out. The observation suggests additional ways to synthesize novel ceramic/polymer architectures using known ATRP technology. The aluminum oxide/polymer composites show improved compatibility with organic solvents and form stable suspensions.

Acknowledgment. The authors are grateful to Air Products and Chemicals, Inc., and U.S. Department of Energy for funding this work.

Supporting Information Available: Kinetics for individual monomers in MMA/BA copolymerization, ^1H NMR spectrum of polymer cleaved from alumina particles, and DSC scan of the composite. This material is available free of charge via the Internet at <http://pubs.acs.org>.

References and Notes

- (1) Romero, P. G. *Adv. Mater.* **2001**, *13*, 163.
- (2) Beecroft, L. L.; Ober, C. K. *Chem. Mater.* **1997**, *9*, 1302.
- (3) Ha, C. S.; Park, H. D.; Frank, C. W. *Chem. Mater.* **2000**, *12*, 839.
- (4) *Hybrid Inorganic–Organic Composites*; Mark, J. E., Lee, C. Y.-C., Bianconi, P. A., Eds.; American Chemical Society: Washington, DC, 1995; Vol. 585.
- (5) Tamaki, R.; Chujo, Y. *Chem. Mater.* **1999**, *11*, 1719.
- (6) Ahmad, Z.; Mark, J. E. *Chem. Mater.* **2001**, *13*, 3320.
- (7) Bergman, J. S.; Chen, H.; Giannelis, E. P.; Thomas, M. G.; Coates, G. W. *Chem. Commun.* **1999**, *21*, 2179.
- (8) Simon, P. F. W.; Ulrich, R.; Spiess, H. W.; Wiesner, U. *Chem. Mater.* **2001**, *13*, 3464.
- (9) Crivello, J. V.; Mao, Z. *Chem. Mater.* **1997**, *9*, 1554.
- (10) Carrado, K. A.; Xu, L. *Chem. Mater.* **1998**, *10*, 1440.
- (11) (a) Wozniak, M. E.; Sen, A. *Chem. Mater.* **1992**, *4*, 753. (b) Nandi, M.; Conklin, J. A.; Salvati, L.; Sen, A. *Chem. Mater.* **1991**, *3*, 201. (c) Nandi, M.; Conklin, J. A.; Salvati, L.; Sen, A. *Chem. Mater.* **1990**, *2*, 772.
- (12) For recent reviews, see (a) Pyun, J.; Matyjaszewski, K. *Chem. Mater.* **2001**, *13*, 3436. (b) Matyjaszewski, K.; Xia, J. *Chem. Rev.* **2001**, *101*, 2921. (c) Kamigaito, M.; Ando, T.; Sawamoto, M. *Chem. Rev.* **2001**, *101*, 3689.
- (13) Werne, T.; Patten, T. E. *J. Am. Chem. Soc.* **2001**, *123*, 7497.
- (14) Mandal, T. K.; Fleming, M. S.; Walt, D. R. *Nano Lett.* **2002**, *2*, 3.
- (15) Stefan, N.; Henrik, B.; Hellmuth, W.; Manfred, L. H. *Angew. Chem., Int. Ed.* **2001**, *40*, 4016.
- (16) Huang, W.; Kim, J.; Bruening, M. L.; Baker, G. L. *Macromolecules* **2002**, *35*, 1175.
- (17) Ziegler, M. J.; Matyjaszewski, K. *Macromolecules* **2001**, *34*, 415.
- (18) Uegaki, H.; Kotani, Y.; Kamigaito, M.; Sawamoto, M. *Macromolecules* **1998**, *31*, 6756.
- (19) Odian, G. *Principles of Polymerization*; Wiley: New York, 1991; p 457.
- (20) Sugimoto, T. *Monodispersed Particles*; Elsevier: New York, 2001; p 192.

MA020809R